GMR
The Original

STARCH/PVA/CuO ELECTROSPUN NANOSCAFFOLDS FROM *Dictyota sp*. EXTRACT: PHYSICOCHEMICAL CHARACTERIZATION AND ANTICANCER ACTIVITY ON HT-29 AND MCF-7 CELLS

Elsa Sharon Emarald Ruban[1], Palchuri Sneha Ananya[2], Balaguru Natarajan[2], Alagendran Subbarayalu[3]*

[1]Saveetha Medical College & Hospital (SMCH), Saveetha Institute of Medical and Technical Sciences (SIMATS), Thandalam, Chennai, Tamil Nadu 602105, India. elsasharon2004@gmail.com
[2]Department of Dermatology, Saveetha Medical College and Hospital, Saveetha Institute of Medical And Technical Sciences (SIMATS), Thandalam, Chennai-602105, Tamil Nadu, India. Email: sneha2000reddy@gmail.com; bala1guru@gmail.com.
[3]Clinical Neuroscience and Phytomedicine Laboratory, Department of Research, Saveetha College of Nursing (SCON), Saveetha Institute of Medical and Technical Sciences (SIMATS), Chennai 602105, Tamil Nadu, India. Email: proteinblg@gmail.com; alagendrans.scon@saveetha.com. ORCID: https://orcid.org/0009-0009-0749-7180.
*Correspondence: proteinblg@gmail.com; alagendrans.scon@saveetha.com (A.S.)

ABSTRACT
This study presents the eco-friendly fabrication of multifunctional starch/PVA electrospun nanoscaffolds incorporated with biogenic copper oxide nanoparticles (CuO NPs) synthesized using *Dictyota* sp. extract via ultrasonication. The phytochemical-assisted CuO NPs exhibited a surface plasmon resonance peak at 270–300 nm in UV-Vis spectroscopy, while Fourier-transform infrared spectroscopy (FTIR) confirmed Cu–O bonding (594–2033 cm^{-1}) and successful integration into the polymer matrix. X-ray diffraction (XRD) revealed a monoclinic CuO phase (JCPDS 48-1548) with high crystallinity, whereas Scanning electron microscopy (SEM) demonstrated uniform nanofiber morphology with well-dispersed NPs. Thermogravimetric analysis (TGA) indicated enhanced thermal stability (residue stable up to 548°C), and Dynamic light scattering (DLS) analysis showed colloidal stability (zeta potential: −20.08 mV; size: 92.8 nm). The nanoscaffolds exhibited potent anticancer activity against HT-29 and MCF-7 cells, with IC50 values of ~12.5 µg/mL—significantly lower than algal extract (IC_{50} ~50 µg/mL) or CuO NPs alone (IC50 ~25 µg/mL). These results underscore the scaffold's dual functionality as a thermally stable, cytotoxic agent, highlighting its potential for biomedical applications.

KEYWORDS: *Dictyota sp.*, Green synthesis, CuO nanoparticles, Starch/PVA/CuO-NPs nanoscaffolds, Anticancer activity.

1. INTRODUCTION

The increasing demand for innovative, multifunctional biomaterials in biomedical applications has sparked significant research into the development of nanostructured scaffolds with enhanced therapeutic efficacy and biocompatibility [1]. Among various biomaterials, starch and polyvinyl alcohol (PVA) have emerged as promising candidates for fabricating electrospun nanofibrous scaffolds due to their biodegradability, excellent film-forming capabilities, and compatibility with biological tissues [2]. Starch, a naturally abundant polysaccharide, offers unique advantages including cost-effectiveness, renewability, and the ability to mimic the extracellular matrix (ECM) structure, thereby supporting cell attachment and proliferation [3]. PVA, a synthetic polymer known for its mechanical strength and water solubility, complements starch by improving the scaffold's structural integrity and processability during electrospinning [4]. The integration of these polymers into hybrid nanofibrous scaffolds provides an ideal platform for further functionalization with bioactive nanomaterials aimed at enhancing their therapeutic potential [5].

Copper oxide nanoparticles (CuO NPs) have recently gained considerable attention due to their remarkable physicochemical properties, including strong antimicrobial, catalytic, and anticancer activities [6]. The nanoscale size of CuO allows for increased surface area and reactivity, which can be exploited to target cancer cells effectively while minimizing adverse effects on healthy tissues [7]. However, conventional chemical methods for synthesizing CuO NPs often involve toxic reagents and harsh conditions, raising concerns about environmental safety and biocompatibility [8]. To address these challenges, green synthesis approaches have been introduced

that utilize natural extracts from plants and marine organisms as reducing and stabilizing agents [9]. These biogenic methods are environmentally friendly, cost-efficient, and impart enhanced biological functionality to the nanoparticles due to the presence of phytochemicals [10].

Marine macroalgae, specifically brown seaweeds such as *Dictyota* species, represent an untapped reservoir of bioactive compounds capable of facilitating the eco-friendly synthesis of metal nanoparticles [11]. *Dictyota* is rich in polysaccharides, polyphenols, flavonoids, and other secondary metabolites that exhibit potent antioxidant and anticancer properties [12]. The ultrasonic-assisted extraction technique further enhances the recovery of these intracellular bioactives by disrupting cell walls through cavitation effects, allowing efficient release without the use of toxic solvents [13]. This approach not only maximizes the yield of reducing agents but also aligns with sustainable processing principles [14]. Incorporating *Dictyota* extract-mediated CuO NPs into starch/PVA nanofibrous scaffolds holds the potential to generate multifunctional materials with synergistic anticancer activity, structural robustness, and controlled release profiles [15].

Electrospinning is a versatile and widely employed technique for fabricating nanofibrous scaffolds with tunable fiber diameters, high surface-to-volume ratios, and porosity resembling natural ECM [16]. These characteristics are crucial for biomedical applications, particularly in tissue engineering and drug delivery, as they facilitate cellular interactions and nutrient transport [17]. The inclusion of CuO NPs within the electrospun matrix can impart additional functionalities such as reactive oxygen species (ROS) generation, which selectively induces apoptosis in cancer cells [18]. Furthermore, the use of starch and PVA as the polymer matrix ensures that the scaffold maintains a biocompatible environment conducive to cell attachment while offering mechanical support [19].

Despite these advantages, challenges remain in optimizing the synthesis conditions and material properties to balance nanoparticle loading, scaffold morphology, and biological efficacy [20]. Ensuring homogeneous dispersion of CuO NPs within the polymeric matrix is critical to avoid agglomeration, which can compromise the mechanical properties and reduce bioavailability [21]. Ultrasonic-assisted biogenic synthesis provides an effective route for producing stable, well-dispersed nanoparticles with controlled size and surface charge, which can be seamlessly integrated into the starch/PVA solution prior to electrospinning [22]. The physicochemical characterization of the resulting nanocomposites—including analyses of morphology, crystallinity, thermal stability, and surface chemistry—is essential to understand the structure-function relationships governing their performance [23].

Cancer remains one of the leading causes of mortality worldwide, and current treatment modalities such as chemotherapy and radiation often suffer from systemic toxicity and drug resistance [24]. The development of novel nanomaterials with targeted anticancer properties is therefore a critical research priority [25]. CuO NPs have demonstrated promising cytotoxic effects against various cancer cell lines by inducing oxidative stress and disrupting mitochondrial function [18]. When embedded within a biocompatible scaffold, these nanoparticles can provide localized and sustained delivery, reducing off-target effects and enhancing therapeutic outcomes [26]. Evaluating the *in vitro* anticancer activity of starch/PVA/CuO nanoscaffolds against human colon (HT-29) and breast (MCF-7) cancer cells provides a relevant model to assess their potential clinical utility [27].

Therefore, this study explores the fabrication of multifunctional electrospun nanoscaffolds composed of starch and PVA, incorporating CuO NPs synthesized via an eco-friendly, ultrasonic-assisted method using *Dictyota* brown macroalgae extract [28]. This innovative combination aims to leverage the biocompatibility and mechanical properties of the polymer blend alongside the bioactivity of CuO NPs, ultimately generating a composite material with promising anticancer properties [29]. Comprehensive physicochemical characterization of the nanoscaffolds and evaluation of their cytotoxicity against cancer cells will shed light on their suitability for advanced biomedical applications [30]. This research contributes to the growing field of marine-derived green nanotechnology and offers new insights into designing sustainable, multifunctional biomaterials for cancer therapy.

2. MATERIALS AND METHODS

2.1 Chemicals and reagents

The brown seaweed *Dictyota* was collected from the coastal waters near Rameswaram, Tamil Nadu, India, and utilized as a renewable source for the green synthesis of CuO NPs. Copper (II) sulfate pentahydrate ($CuSO_4 \cdot 5H_2O$), analytical grade, was the copper precursor. PVA with an approximate molecular weight of 115,000 g/mol and starch were chosen as biocompatible scaffold materials. Electrospinning procedures employed the HOLMARC HO-NFES-040 system. All chemicals and solvents were sourced from Sigma-Aldrich and Merck with analytical grade purity to guarantee consistency and accuracy. Characterization techniques included UV-Vis spectroscopy, Fourier-transform infrared spectroscopy (FTIR), X-ray diffraction (XRD), scanning electron microscopy (SEM), dynamic light scattering (DLS), zeta potential, and thermogravimetric analysis (TGA). The *in vitro* anticancer properties were assessed according to established protocols.

2.2 Collection and preparation of marine algae

Fresh *Dictyota* specimens were manually gathered from the intertidal zone of the Rameswaram shoreline. After collection, samples were kept chilled to preserve their bioactive components. The biomass was rinsed thoroughly with running tap water to remove sediments and epiphytes, followed by multiple rinses with distilled water to eliminate salt and residual debris. Around 100 g of the cleaned algae were chopped into smaller fragments and air-dried at ambient temperature for 14 days. The dried material was subsequently ground into a fine powder using a mechanical grinder and stored in sealed containers for later extraction and nanoparticle synthesis.

2.3 Ultrasonic extraction of bioactive compounds

Two grams of the dried algal powder were dispersed in 50 mL of Milli-Q water within a 100 mL borosilicate beaker. This suspension underwent ultrasonic-assisted extraction in a LABQUEST ultrasonic cleaner (Borosil; Serial No. 941032329018) maintained at 60°C for 45 minutes to enhance intracellular metabolite release via cell disruption. The mixture was then filtered through sterile Whatman No. 1 filter paper to separate solids. The clarified extract was stored at 10°C for subsequent use, and a portion was lyophilized to extend shelf-life and yield a dry extract appropriate for nanoparticle synthesis [31, 32].

2.4 Eco-friendly synthesis of CuO NPs

CuO NPs were synthesized by combining 50 mL of 0.1 M $CuSO_4 \cdot 5H_2O$ with 10 mL of *Dictyota* extract (10 mg/mL) in a 5:1 volume ratio. The mixture was magnetically stirred at 650 rpm and maintained at 60°C for 2 hours. A visible color transition from deep blue to bluish-green signified nanoparticle formation driven by phytochemicals in the extract. The product was washed thrice with double-distilled water to remove residual biomolecules and then freeze-dried for 48 hours to obtain CuO nanopowder for further experimentation [33].

2.5 Synthesis of starch/PVA/CuO nanofibrous scaffolds

A 15% (w/w) aqueous PVA solution was prepared by dissolving PVA in Milli-Q water under continuous stirring at 50°C. After complete dissolution, 100 mg each of starch and CuO nanoparticles were added and stirred at 50°C for 2.5 hours to achieve homogeneity. The resultant mixture was loaded into a syringe equipped with a 0.84 mm stainless steel needle. Electrospinning was conducted using the HOLMARC HO-NFES-040 apparatus at 11.5 kV applied voltage, a 12.3 cm gap between the needle and collector, and a feed rate of 0.4 mL/h. Electrospinning lasted 6 to 8 hours at room temperature, producing nanofibrous mats subsequently stored in a desiccator for characterization and biological testing [2, 34, 35].

2.6 Physicochemical characterization

2.6.1 UV-vis spectroscopy

UV-Vis spectral analysis of the algal extract, synthesized CuO NPs, and nanocomposite scaffolds was performed using a VIS SPEC V-730 spectrophotometer. Absorption spectra were recorded between 200 and 800 nm with deionized water serving as the blank. The presence of absorption peaks in the 270–300 nm range indicated surface plasmon resonance (SPR), confirming CuO NP formation and integration into scaffolds [36].

2.6.2 FTIR spectroscopy

FTIR spectra of the algal extract, nanoparticles, and scaffolds were recorded using a PerkinElmer Spectrum Two instrument equipped with an ATR accessory. Spectra were acquired over 4000–400 cm^{-1} at a resolution of 4 cm^{-1}, averaged from 64 scans. The characteristic peaks corresponding to hydroxyl, carbonyl, amide, and metal-oxygen groups confirmed bioactive molecule presence and nanoparticle incorporation [37].

2.6.3 XRD analysis

XRD patterns were obtained using a Bruker D8 Advance diffractometer employing CuKα radiation ($\lambda = 1.5406$ Å) at 40 kV and 40 mA. Data were collected from 2θ values ranging 5° to 90° with a step size of 0.029649°. Sharp diffraction peaks characteristic of monoclinic CuO confirmed successful nanoparticle synthesis, whereas peak broadening in scaffold samples indicated polymer embedding [38].

2.6.4 SEM analysis

Morphological examination was conducted with a JEOL JSM-IT800 NANO SEM. Samples were gold sputter-coated prior to imaging. Micrographs revealed uniform fibrous structures, consistent fiber diameters, and homogeneous CuO NP distribution, confirming effective electrospinning fabrication [39].

2.6.5 TGA

Thermal stability was assessed using a PerkinElmer TGA 8000. Approximately 5 mg of sample was heated from room temperature to 550°C at 15°C/min under a nitrogen atmosphere. Weight loss profiles reflected moisture evaporation, polymer degradation, and enhanced thermal stability attributed to CuO NP incorporation [40].

2.6.6 Particle size and zeta potential

Nanoparticle size distribution and surface charge were analyzed using a Malvern Zetasizer Ultra. Zeta potential values above ±30 mV indicated excellent colloidal stability, minimizing aggregation and favoring biomedical applications [41]. All data have been deposited in the Mendeley Data repository (DOI: 10.17632/xtwhbc25hj.2) for verification.

2.7 *In Vitro* anticancer activity

2.7.1 Cell lines procurement and culture

Human colorectal adenocarcinoma (HT-29) and breast cancer (MCF-7) cell lines were procured from the National Center for Cell Science (NCCS), Pune, India. Cells were cultured in Minimum Essential Medium (MEM) supplemented with 10% fetal bovine serum (FBS) and maintained at 37°C in a humidified 5% CO_2 atmosphere [42].

2.7.2 Cell viability assay using MTT

HT-29 and MCF-7 cells were seeded in 96-well plates at 5×10^5 cells/well and incubated overnight for adherence. Cells were then exposed to varying concentrations (6.25, 12.5, 25, 50, and 100 µg/mL) of algal extract, CuO NPs, and starch/PVA/CuO nanoscaffolds in triplicate and incubated for 24 hours at 37°C with 5% CO_2. Post-treatment, 20 µL of MTT solution was added per well and incubated for 4 hours. Formazan crystals were solubilized using 200 µL DMSO, and absorbance was measured at 570 nm. Experiments were performed thrice independently. Mean absorbance values with standard deviations were calculated [43].

2.8 Statistical analysis

Data were analyzed using SPSS v25.0 and GraphPad Prism v9.0. Triplicate experimental results are expressed as mean ± standard deviation. One-way ANOVA followed by Tukey's or Dunnett's post hoc tests were used to compare groups, with significance set at $p < 0.05$. Pearson's correlation assessed variable relationships. Normality was checked using the Shapiro–Wilk test; non-normal data were log-transformed. Statistical interpretations were performed within a 95% confidence interval [44].

3. RESULTS

3.1. UV–visible spectroscopy

UV–Visible spectroscopy analysis (Fig. 1) was conducted using a JASCO V-730 spectrophotometer within the 200–800 nm wavelength range to examine the *Dictyota* extract alongside the synthesized CuO NPs. The algal extract displayed a broad absorption band peaking at 337 nm (absorbance = 1.482), which indicates the presence of phytochemicals such as polyphenols. These biomolecules are believed to facilitate the reduction and stabilization processes during nanoparticle synthesis. The CuO NPs exhibited a pronounced absorption peak between 270 and 300 nm, attributed to SPR, a hallmark of nanoparticle optical properties. Furthermore, the CuO NPs showed markedly higher absorbance values (2.369 at 800 nm) that diminished toward shorter wavelengths, consistent with typical optical characteristics of metal oxides. These spectral changes confirm successful nanoparticle synthesis and suggest the active role of *Dictyota*-derived phytoconstituents in their formation and stabilization [45].

3.2. FTIR analysis

FTIR (Fig. 2) was employed to characterize functional groups in the CuO NPs and CuO-loaded starch/PVA scaffolds. The CuO NPs revealed absorption peaks at 2033.36, 1640.64, and 594.02 cm^{-1}, corresponding to Cu–O bond stretching vibrations, thus verifying copper oxide formation. Additional bands at 767.66 and 469.77 cm^{-1} further corroborate copper–oxygen interactions. The composite scaffold exhibited major absorption signals at 3289.72 cm^{-1} (O–H stretching), 1426.07 cm^{-1} (C–H bending), and 110.59 cm^{-1} (C–O–C vibrations), representing the characteristic chemical features of starch and PVA polymers. Importantly, peaks detected between 600 and 400 cm^{-1} confirm the successful embedding of CuO NPs into the polymer framework. These results imply that the nanoparticles were incorporated without significantly altering the scaffold's chemical structure [46].

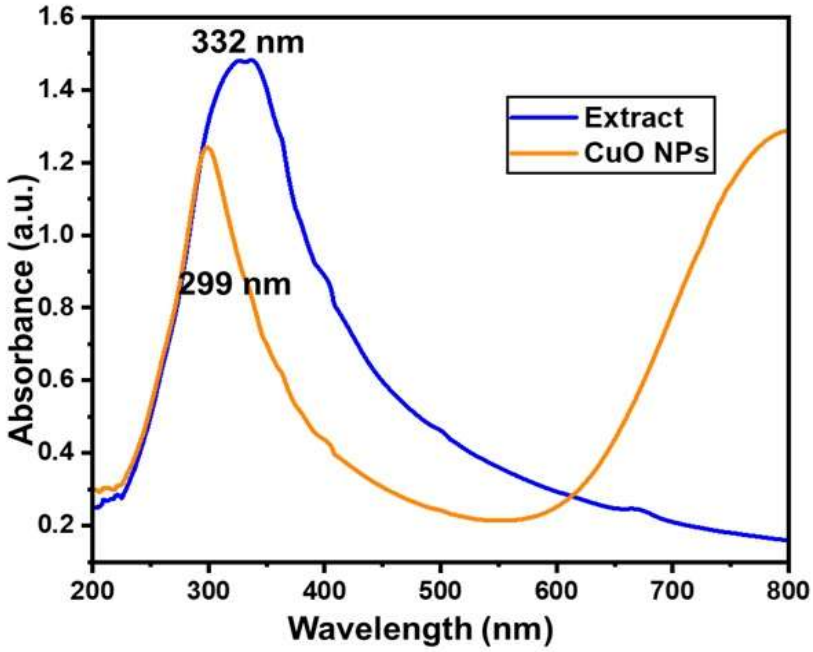

Fig. 1. UV–Visible spectral profiles of algal extract and CuO NPs.

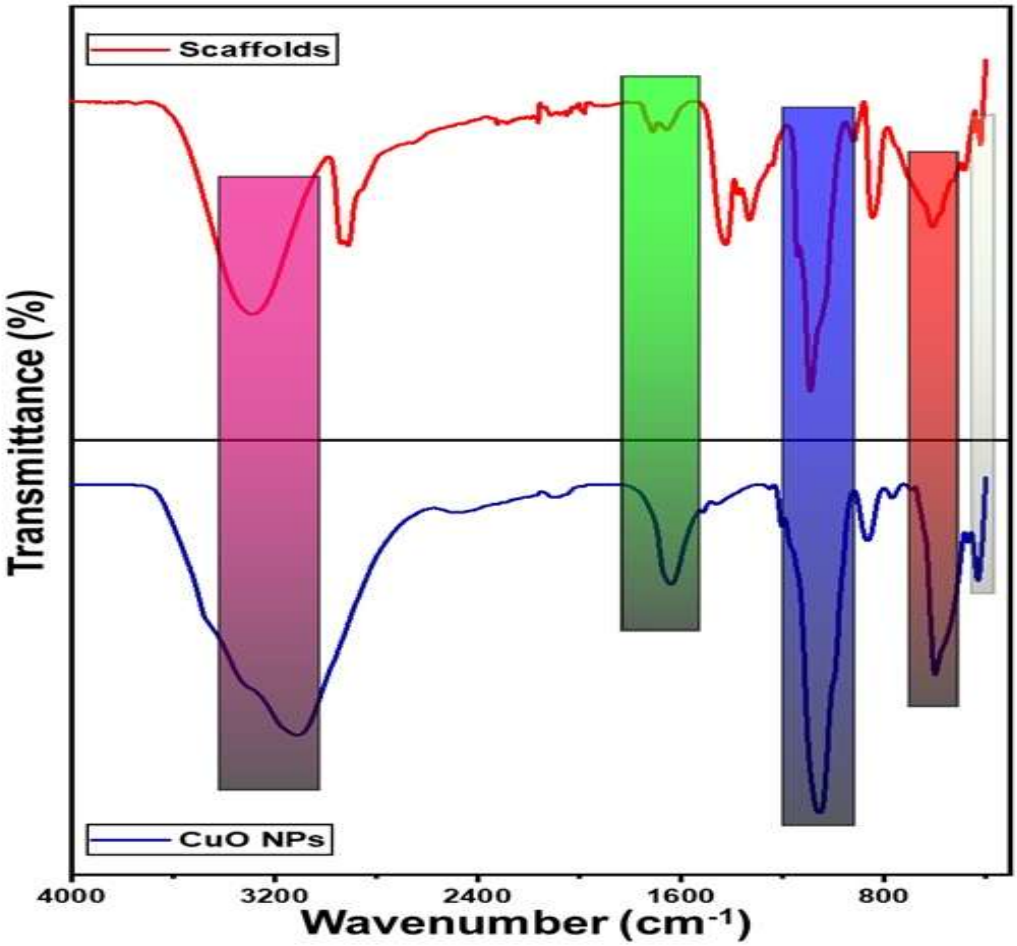

Fig. 2. FTIR spectra of CuO NPs and their incorporation into nanoscaffolds.

3.3. XRD analysis

XRD analysis (Fig. 3) was utilized to assess the crystalline properties of the synthesized CuO NPs and their integration into the starch/PVA matrix. The CuO NPs displayed distinct diffraction peaks at 2θ values of 14.03°,

15.60°, 16.25°, and 24.17°, matching the monoclinic CuO phase as per JCPDS card No. 48-1548. The strongest peak at 24.17° (d-spacing of 3.68 Å) indicated a high degree of crystallinity. The starch/PVA scaffold presented broad diffraction peaks at 21.35° and 29.30°, typical of semicrystalline polymers. Additional weaker reflections at 35.78° and 48.52° provided evidence for successful CuO NP incorporation. Peak broadening (FWHM between 0.1° and 0.6°) suggests a decrease in crystallinity caused by nanoparticle-polymer interactions. Collectively, the data confirm effective nanoparticle embedding without disrupting the overall phase, essential for biomedical applications [47].

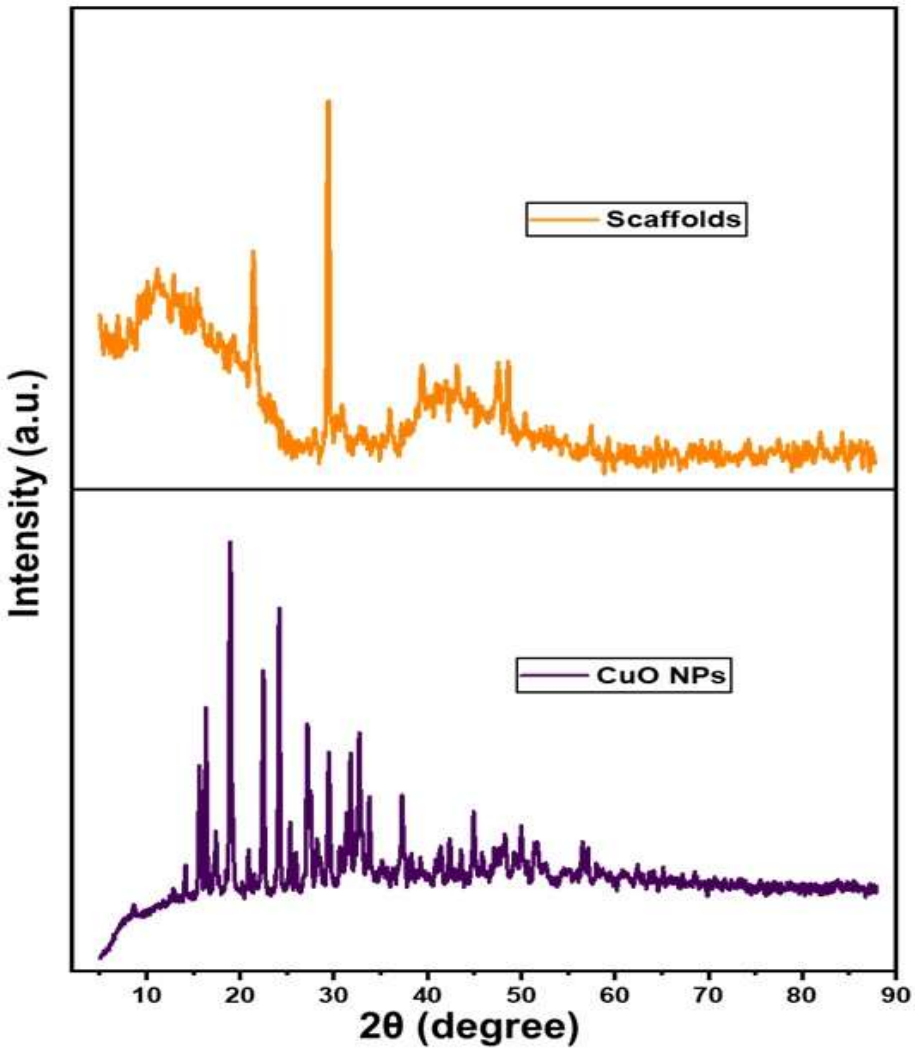

Fig. 3. XRD patterns of synthesized CuO NPs and CuO-loaded scaffolds.

3.4. SEM analysis

SEM (Fig. 4) was employed to observe the surface morphology and nanoparticle distribution within the electrospun starch/PVA nanofiber scaffolds. The CuO NPs appeared predominantly spherical with minor agglomerations, likely due to surface energy effects. The nanofibers exhibited a uniform and well-aligned fibrous structure at the nanoscale. Bright spots along the fibers corresponded to CuO NPs, confirming their successful distribution throughout the scaffold. The fiber surfaces were smooth with slight textural features, indicating good compatibility between CuO NPs and the polymer matrix. Minimal bead formation and consistent fiber diameters reflected optimized electrospinning conditions. These morphological results validate the homogeneous dispersion of CuO NPs, preserving scaffold integrity for potential biomedical use [48].

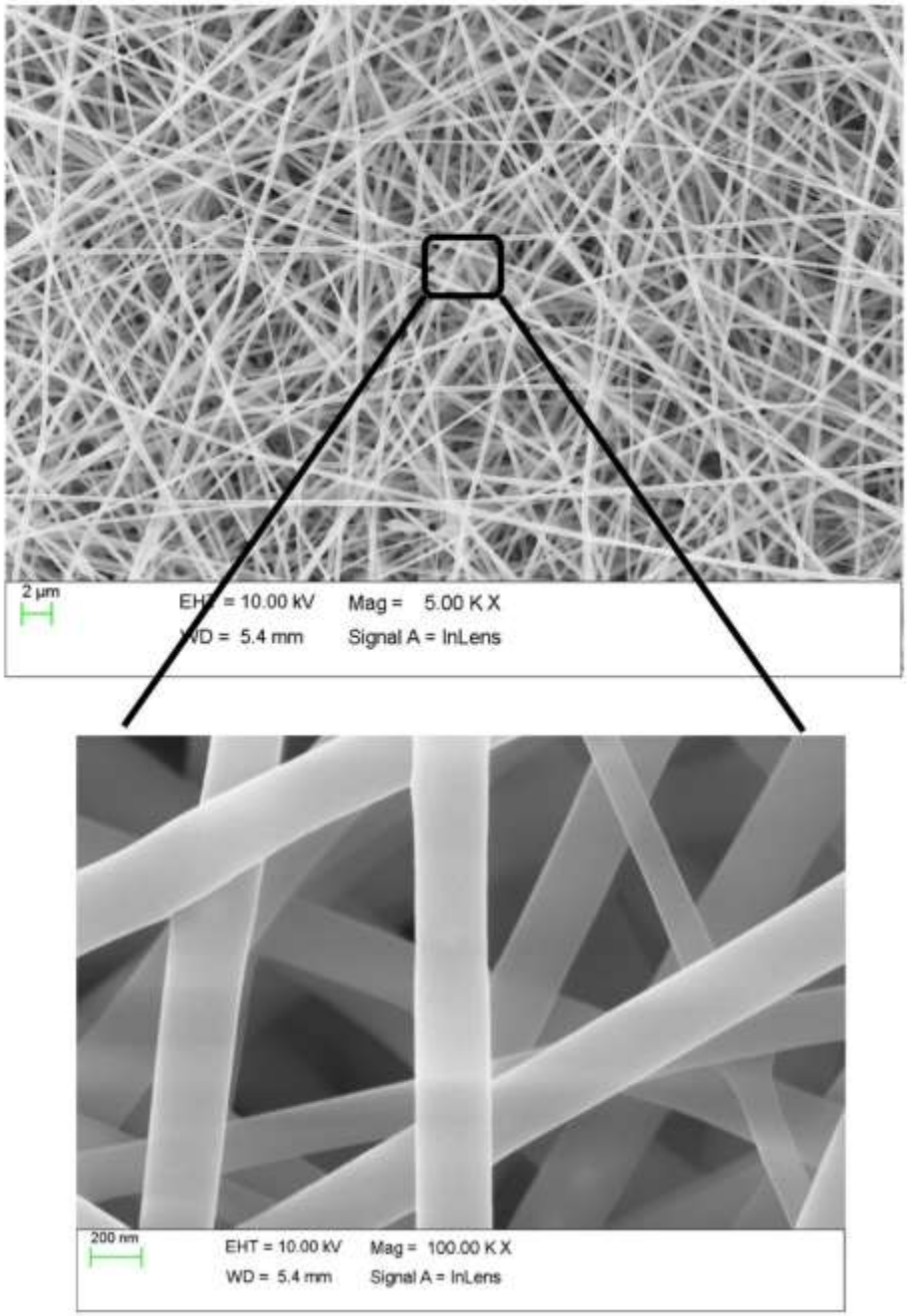

Fig. 4. SEM analysis of fabricated starch/PVA/CuO-NPs nanoscaffolds.

3.5. TGA

TGA of CuO NP-incorporated nanofiber scaffolds was performed under nitrogen atmosphere (Fig. 5) to evaluate thermal stability. An initial weight loss of 7.30% occurred below 101.7°C, attributed to evaporation of adsorbed moisture. Major thermal degradation happened between 234.95°C and 377.09°C, with a peak at 324.79°C, representing decomposition of the starch/PVA matrix and accounting for 37.37% mass loss. Beyond 400°C, a gradual mass decrease indicated carbonaceous residue formation alongside the thermally stable CuO nanoparticles. The residue remained stable up to 548.4°C, demonstrating enhanced thermal resistance imparted by CuO NPs. These findings suggest that CuO inclusion improves the scaffold's heat tolerance, beneficial for biomedical and industrial environments requiring elevated thermal durability [49].

3.6. Zeta potential and particle size analysis

DLS and zeta potential measurements were performed to analyze particle size distribution and colloidal stability of the synthesized CuO NPs. The average hydrodynamic diameter was 92.8 nm (Fig. 6), with a polydispersity index (PDI) of 0.688, indicating moderate size variability. Zeta potential analysis (Fig. 7) revealed a mean surface charge of −20.08 mV, with peaks at −37.52 mV and −16.29 mV. The relatively high negative zeta potential suggests adequate electrostatic repulsion to prevent nanoparticle aggregation, ensuring colloidal stability. The

conductivity was measured at 0.0343 mS/cm, and the quality factor was 6.538, reflecting high measurement reliability. These parameters confirm the nanoparticles possess good dispersion and electrostatic stability, suitable for biomedical formulations requiring consistent nanoparticle performance in aqueous systems [50].

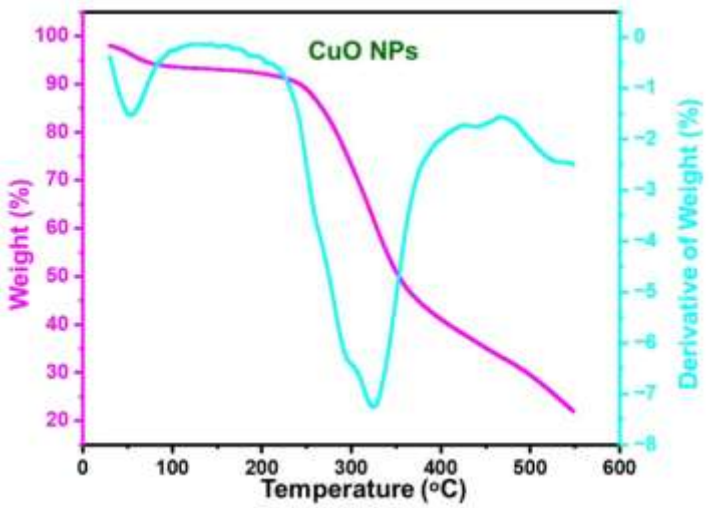

Fig. 5. Thermal degradation behavior of CuO-incorporated nanoscaffolds.

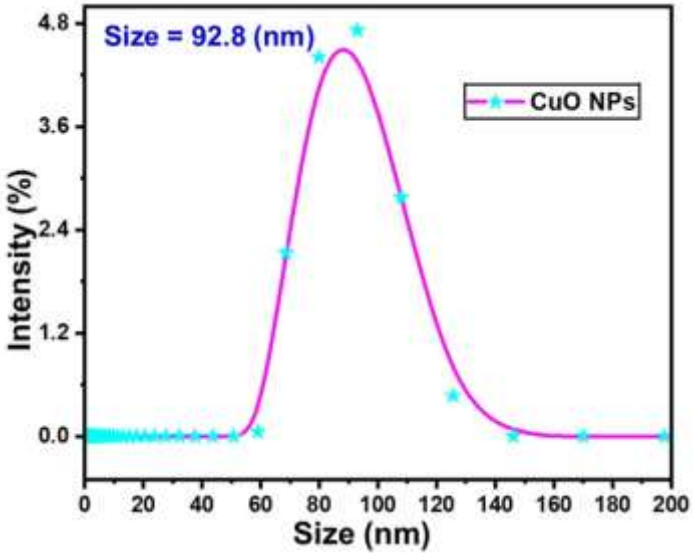

Fig.6. DLS particles size analysis of CuO NPs

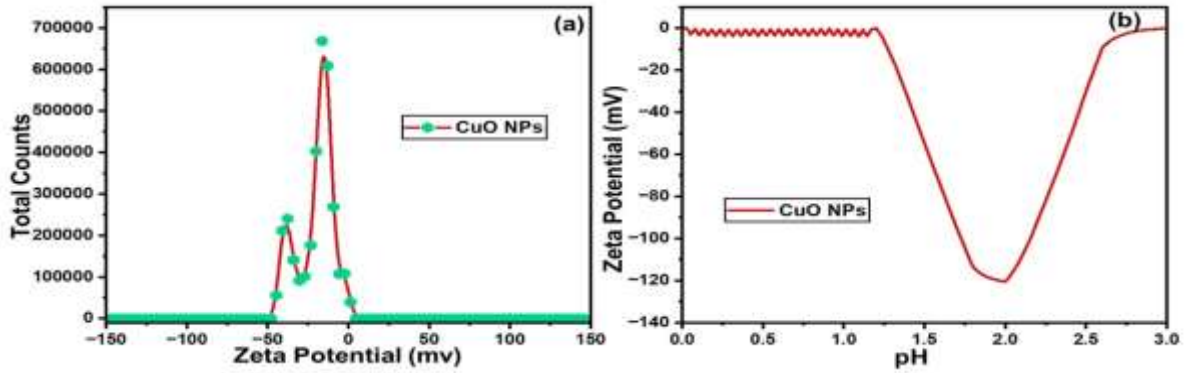

Fig.7. Zeta-potential analysis of CuO NPs

3.7. Evaluation of *in vitro* anticancer activity

The *in vitro* anticancer activity of algal extract, CuO NPs, and starch/PVA/CuO-NPs nanoscaffolds was evaluated against HT-29 (colon adenocarcinoma) and MCF-7 (breast cancer) cell lines using the MTT assay (Fig. 8). The results demonstrated a concentration-dependent reduction in cell viability for all tested compounds.

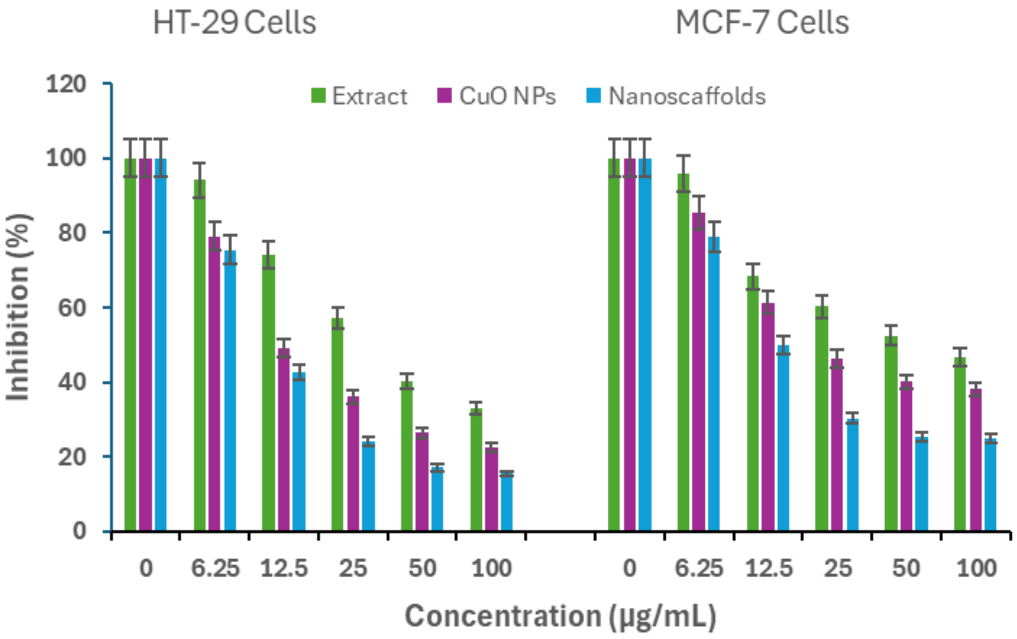

Fig.8. Anticancer activity analysis of algal extract, CuNPs and starch/PVA/CuONPs nanoscaffolds

Against HT-29 cells, the algal extract showed moderate cytotoxicity, with cell viability decreasing from 94.1% at 6.25 µg/mL to 32.85% at 100 µg/mL, yielding an estimated IC50 of approximately 50 µg/mL. CuO NPs exhibited stronger activity, reducing viability from 79.1% to 22.43% over the same concentration range, with an IC50 of about 25 µg/mL. The starch/PVA/CuO-NPs nanoscaffolds displayed the most potent effect, lowering viability from 75.5% to 15.48% and achieving an IC50 of roughly 12.5 µg/mL, indicating superior anticancer potential.

Similar trends were observed in MCF-7 cells. The algal extract reduced viability from 95.9% to 46.65%, with an IC50 near 50 µg/mL. CuO NPs again showed intermediate efficacy (85.4% to 38.07% viability; IC50 ~25 µg/mL), while the nanoscaffolds demonstrated the highest cytotoxicity (79.0% to 25.02% viability; IC50 ~12.5 µg/mL).

These findings highlight the enhanced anticancer activity of the starch/PVA/CuO-NPs nanoscaffolds compared to individual components, suggesting their promise as a therapeutic candidate. The consistent IC50 values across both cell lines further validate the nanoscaffolds' potency, warranting further investigation into their mechanisms and *in vivo* efficacy [51].

4. DISCUSSION

The present study successfully synthesized CuO NPs using *Dictyota* algal extract, incorporated them into starch/PVA nanofibrous scaffolds, and evaluated their physicochemical characteristics alongside *in vitro* anticancer efficacy. The results from diverse analytical techniques provide comprehensive insight into the material's properties and their implications for biomedical applications.

The UV–Visible spectroscopy findings clearly establish the role of *Dictyota* extract as a bioreductant and stabilizing agent in the green synthesis of CuO NPs. The broad absorption peak at 337 nm in the algal extract is indicative of polyphenolic compounds, which are known for their electron-donating capability facilitating metal ion reduction. The distinct SPR peak observed in the 270–300 nm range for CuO NPs is a hallmark of nanoparticle formation, corroborating successful synthesis. Moreover, the elevated absorbance at longer wavelengths (800 nm) reflects the intrinsic optical properties of copper oxides, often attributed to electronic transitions in the Cu–O lattice. This shift in spectral features from the extract to the nanoparticles underscores the phytochemicals' active involvement in nucleating and stabilizing the CuO nanostructures, preventing aggregation through surface capping effects [52, 53].

FTIR spectroscopy further substantiated the successful formation of CuO NPs and their integration into the starch/PVA scaffold. The characteristic Cu–O stretching vibrations detected at multiple wavenumbers align with previously reported copper oxide spectra, confirming the chemical identity of the synthesized nanoparticles. Importantly, the polymeric scaffold retained its primary chemical functionalities—such as hydroxyl and ether groups—after nanoparticle incorporation, as shown by the preserved absorption peaks of starch and PVA. This implies that the biopolymer matrix effectively accommodates the CuO NPs without compromising its intrinsic chemical structure. The presence of Cu–O vibrational bands within the scaffold's spectrum affirms a strong nanoparticle-polymer interaction, likely through physical embedding or weak bonding, which can enhance the scaffold's stability and functional properties [54, 55].

XRD analysis illuminated the crystalline nature of the CuO NPs and their impact on the composite scaffold's structural characteristics. The diffraction peaks corresponded well with the monoclinic CuO phase, indicating high purity and crystallinity. The starch/PVA scaffold exhibited typical broad peaks, characteristic of semi-crystalline polymers, which became broader and less intense upon CuO NP incorporation. This peak broadening suggests that the embedded nanoparticles disrupt polymer chain packing to some extent, reducing overall crystallinity—a phenomenon frequently reported in nanoparticle-polymer composites. Notably, the absence of additional peaks or phase shifts demonstrates that CuO NPs were integrated without altering the fundamental crystalline phases of either component, an essential aspect for preserving mechanical and functional integrity in biomedical scaffolds [56-59].

Surface morphology observations via SEM provided visual confirmation of nanoparticle distribution and scaffold microstructure. The spherical shape of CuO NPs with minor aggregation indicates controlled synthesis, though some degree of agglomeration is expected due to surface energy interactions. The nanofibrous scaffold morphology was notably uniform and aligned, reflecting optimized electrospinning conditions. Bright, discrete spots along the fibers confirmed homogeneous CuO NP dispersion, crucial for consistent biological activity and mechanical reinforcement. The smooth yet slightly textured fiber surfaces suggest favorable interactions between the nanoparticles and the polymeric matrix, potentially improving scaffold toughness and bioactivity. Minimal bead formation further supports the stability of the electrospinning process and the compatibility of the CuO NP-polymer blend [60-63].

TGA revealed that CuO NPs enhance the thermal stability of the starch/PVA scaffold. The initial weight loss due to moisture evaporation is typical in hydrophilic biopolymers. The major degradation phase corresponds to polymer decomposition, which was significantly influenced by the presence of CuO NPs, evident from the elevated decomposition temperature and increased residual mass at higher temperatures. This improved thermal resistance can be attributed to the nanoparticles acting as heat sinks and barrier elements, delaying polymer chain degradation. Enhanced thermal stability is advantageous for biomedical materials, as it broadens their potential applications in environments requiring sterilization or exposure to elevated temperatures [64-67].

DLS and zeta potential measurements provided key insights into nanoparticle size and colloidal stability. The hydrodynamic diameter near 93 nm confirms the nanoscale dimension appropriate for biomedical use, where small size facilitates cellular uptake and interaction. The polydispersity index indicates moderate size uniformity, which could be further optimized but is acceptable for functional applications. The moderately high negative zeta potential indicates strong electrostatic repulsion among particles, effectively preventing aggregation and sedimentation in aqueous media. This colloidal stability is critical for maintaining consistent nanoparticle behavior in biological environments, ensuring reproducible therapeutic effects and minimizing toxicity caused by large aggregates [68].

Finally, the *in vitro* anticancer assays demonstrated the superior cytotoxicity of starch/PVA/CuO NP nanoscaffolds compared to individual components against both colon (HT-29) and breast (MCF-7) cancer cell lines. The dose-dependent decrease in cell viability suggests effective cellular uptake and bioactivity of the nanoscaffolds. The lower IC50 values for the nanoscaffolds relative to algal extract or CuO NPs alone highlight the synergistic effect of nanoparticle incorporation into a biocompatible polymer matrix, which likely enhances bioavailability and sustained release of cytotoxic agents. These results support the potential of CuO NP-loaded scaffolds as promising anticancer therapeutic platforms, combining the benefits of green synthesis, nanotechnology, and polymer engineering. Further mechanistic studies are warranted to elucidate pathways of cytotoxicity, including ROS generation and apoptosis induction, along with *in vivo* evaluations to confirm clinical relevance [69].

Finally, this study establishes a robust, green synthetic route for CuO NPs using *Dictyota* extract and demonstrates their successful incorporation into starch/PVA nanofibers with enhanced physicochemical and biological properties. The multifunctional nature of the resulting nanocomposite scaffold, combining thermal stability, structural integrity, and potent anticancer activity, positions it as a compelling candidate for advanced biomedical applications.

5. CONCLUSION

In conclusion, this study successfully demonstrated the green synthesis of CuO NPs using *Dictyota* algal extract, highlighting the extract's dual role as a reducing and stabilizing agent. The incorporation of CuO NPs into starch/PVA nanofibrous scaffolds was confirmed through comprehensive characterization techniques, including UV–Visible spectroscopy, FTIR, XRD, SEM, and thermal analysis. These analyses revealed effective nanoparticle formation, stable integration within the polymer matrix, and enhanced thermal stability of the composite scaffolds. Moreover, the nanoscaffolds exhibited uniform morphology and maintained good colloidal stability, essential for biomedical applicability. Importantly, the starch/PVA/CuO-NP scaffolds showed superior anticancer activity against both colon and breast cancer cell lines compared to the individual components, emphasizing their potential as effective therapeutic agents. Collectively, the findings underscore the promise of these biocompatible

nanocomposite scaffolds for future cancer therapy applications, warranting further in-depth biological and *in vivo* investigations to fully explore their clinical potential.

Ethics declaration: Not Applicable

Data Availability Statement: The full dataset of physiochemical characterization associated with this work is published in Mendeley Data (doi: 10.17632/xtwhbc25hj.2). **Disclosure:** The material characterization data and figures (e.g., UV, SEM, FTIR, XRD, TGA, Zeta Potential and particle sizer) presented here were generated from a common dataset and are being reused across multiple related studies on nanomaterials. All biological and environmental analyses and conclusions are original to each manuscript.

Conflicts of Interest: The authors declare no conflicts of interest.

REFERENCES

[1] Surendran N, Raju MV, Chandrasekaran MK, Ahalliya RM, Palanisamy CP, Chandrasekaran G, Kanniappan GV. Physicochemical characterization of starch from Maranta arundinacea L.(arrowroot) rhizomes and its inhibition of COX-2: In vivo validation. Bioactive Carbohydrates and Dietary Fibre. 2025; 33: 100465.

[2] Kannappan P, Chandrasekaran MK, Raju MV, Gopalakrishnan S, Dhamodharan P, Ahalliya RM, Palanisamy CP, Raju B, Kanniappan GV. Exploring the anticancer potential of Jerantinine A from Tabernaemontana coronaria against prostate, breast, and ovarian cancers: a computational approach. Journal of Complementary and Integrative Medicine. 2025; 22(02): 363-372.

[3] Pei J, Kumarasamy RV, Jayaraman S, Kanniappan GV, Long Q, Palanisamy CP. Quercetin-functionalized nanomaterials: Innovative therapeutic avenues for Alzheimer's disease management. Ageing Research Reviews. 2025; 104: 102665.

[4] Jayaraman S, Prasad M, Natarajan SR, Krishnamoorthy R, Alshuniaber MA, Gatasheh MK, Veeraraghavan VP, Rajagopal P, Palanisamy CP. Molecular mechanisms underlying the effects of beta-sitosterol on TGF-β1/Nrf2/SIRT1/p53-mediated signaling in the kidney of a high-fat diet and sucrose-induced type-2 diabetic rat. Chemico-Biological Interactions. 2025; 411: 111443.

[5] Huang Y, Guo H, Liu Y, Jin W, Palanisamy CP, Pei J, Oz F, El-Aty AMA. Effects of Natural Polysaccharides on the Gut Microbiota Related to Human Metabolic Health. Molecular Nutrition & Food Research. 2025; e202400792.

[6] Prabhakaran P, Palanisamy CP, Shanmugam A, Damodharan P, Swaminathan H, Devaraj D, Ahalliya RM, Kanniappan GV. Isolation, structural characterization, and molecular docking studies on the bioactive compound from n-Hexane extract of Emilia sonchifolia (L.) DC against the pancreatic cancer target Aurora 2 Kinase. Journal of Complementary and Integrative Medicine. 2024; 22(1): 0290.

[7] Jiang H, Kumarasamy RV, Pei J, Raju K, Kanniappan GV, Palanisamy CP. Integrating engineered nanomaterials with extracellular vesicles: Advancing targeted drug delivery and biomedical applications. Frontiers in Nanotechnology. 2024; 6: 1513683.

[8] Guo H, Liu Y, Wan T, Song D, Palanisamy CP, Geng J, Pei J, Özmen S, El-Aty AMA. Toward personalized cancer management: Role of precision nutrition–diet interventions. Journal of Functional Foods. 2024; 123: 106584.

[9] Natarajan SR, Krishnamoorthy R, Alshuniaber MA, Al-Anazi KM, Farah MA, Rajagopal P, Palanisamy CP, Veeraraghavan VP, Jayaraman S. Identification of FOXM1 as a novel protein biomarker and therapeutic target for colorectal cancer progression: Evidence from immune infiltration and bioinformatic analyses. International Journal of Biological Macromolecules. 282 (Part 4): 137201.

[10] Rajendran MS, Jayaraman S, Khan JM, Jasmine S, Prabhakaran RK, Raju MV, Chandrasekaran MK, Ahalliya RM, Kannappan P, Palanisamy CP, Kanniappan GV. Investigating the colon toxicity and carcinogenic role of monosodium glutamate compared with Dimethylhydrazine in male Wistar rats: Exploring the link to childhood colon cancer risk. Journal of King Saud University - Science. 2024; 36(11): 103507.

[11] Kumarasamy RV, Natarajan P, Umapathy VR, Roy JR, Rab SO, Saeed M, Panagal M, Mironescu M, Srinivasan GP, Palanisamy CP. Clinical Applications and Therapeutic Potentials of Advanced Nanoparticles: A Comprehensive Review on Completed Human Clinical Trials. Frontiers in Nanotechnology. 2024; 6:1479993.

[12] Ganesan A, Kumar NG, Natarajan PM. Anticancer activity of silver nanoparticles synthesized from aqueous leaf extract of Solanum trilobatum (Purple fruit pea eggplant) on human oral cancer cells. Journal of Herbmed Pharmacololgy. 2024; 13(2): 260-268.

[13] Natarajan PM, Swamikannu B, Sivaraman NM, Stylin AGSQ. Prevention of Oral Cancer: A Comprehensive Guide. Journal of Pharmacy and Bioallied Sciences. 2024; 16(5): S4239-S4241.

[14] Umapathy V, Dhanavel A, Kesavan R, Natarajan PM, Bhuminathan S, Vijayalakshmi P. Anticancer Potential of the Principal Constituent of Piper nigrum, Piperine: A Comprehensive Review. Cureus. 2024; 16(2): e54425.
[15] Umapathy VR, Swamikannu B, Natarajan PM, Devi R, Nandini MS, Vimalarani, Vijayalakshmi P. In Silico Molecular Docking of Ocimum sanctum Phytochemicals: Targeting Key Biomarkers in Oral Cancer. Journal of Pharmacy and Bioallied Sciences. 2024; 16(5): S4792-S4799.
[16] Natarajan PM, Bhuminathan S, Rajan R, Bindu K, Loganathan K, Veerakumar R. The Crucial Role of Smoking Cessation in Preventing Oral Cancer. Journal of Pharmacy and Bioallied Sciences. 2024; 16(5): S4245-S4247.
[17] Swamikannu B, Umapathy VR, Natarajan PM, Nandini MS, Stylin AGSQ, Vimalarani V, Rajinikanth S. Unlocking the Therapeutic Benefits of Artemisia Annua: A Comprehensive Overview of its Medicinal Properties. Journal of Pharmacy and Bioallied Sciences. 2024; 16(5): S4248-S4253.
[18] Natarajan PM. Computational Studies on Recent Congeners of Fluoroquinolones and Nitroimidazoles for Their Use in Periodontal Therapy. Journal of Pharmacy and Bioallied Sciences. 2024; 16(5): S4731-S4740.
[19] Yadalam PK, Arumuganainar D, Natarajan PM, Ardila CM. Artificial intelligence-powered prediction of AIM-2 inflammasome sequences using transformers and graph attention networks in periodontal inflammation. Scientific Reports. 2025; 15: 8733.
[20] Yadalam PK, Chatterjee S, Natarajan PM, Ardila CM. Comparison of light gradient boosting and logistic r egression for interactomic hub genes in Porphyromonas gingivalis and Fusobacterium nucleatum-induced periodontitis with Alzheimer's disease. Frontiers in Oral Health. 2025; 6:1463458.
[21] Natarajan PM, Bhuminathan S, Leela B, Bindu K, Loganathan K, Ramachandran V. Smoking and its Role in Oral Cancer. Journal of Pharmacy and Bioallied Sciences 16(5): S4242-S4244.
[22] Yadalam PK, Natarajan PM, Ardila CM. Variational graph autoencoder for reconstructed transcriptomic data associated with NLRP3 mediated pyroptosis in periodontitis. Scientific Reports. 2025; 15: 1962.
[23] Jin W, Pei JJ, Roy JR, Jayaraman S, Ahalliya RM, Kanniappan GV, Mironescu M, Palanisamy CP. Comprehensive review on single-cell RNA sequencing: A new frontier in Alzheimer's disease research. Ageing Research Reviews. 2024; 274: 102454.
[24] Pei J, Palanisamy CP, Jayaraman S, Natarajan PM, Umapathy VR, Roy JR, Panagal M, Jayaraman S. Curcumin-loaded polymeric nanomaterials as a novel therapeutic strategy for Alzheimer's disease: A comprehensive review. Ageing Research Reviews. 2024; 99: 102393.
[25] Pei J, Palanisamy CP, Jayaraman S, Natarajan PM, Umapathy VR, Roy JR, Thalamati D, Ahalliya RM, Kanniappan GV, Mironescu M. A comprehensive review on starch-based Sustainable Edible Films Loaded with Bioactive Components for Food Packaging. International Journal of Biological macromolecules. 2024; 274 (Part-1): 133332.
[26] Palanisamy CP, poompradub S, Sansanaphongpricha K, Subramani K, Sonsudin F. Increased expression levels of PDGF and VEGF magnify the wound healing potential facilitated by biogenic synthesis of silver nanoparticles. Nano-Structures & Nano-Objects. 2024; 39: 101236.
[27] Pei J, Palanisamy CP, Jayaraman S, Natarajan PM, Umapathy VR, Roy JR, Thalamati D, Ahalliya RM, Kanniappan GV, Mironescu M. Proteomics Profiling of Extracellular Vesicle for Identification of Potential Biomarkers in Alzheimer's Disease: A Comprehensive Review. Ageing Research Reviews. 2024; 99: 102359.
[28] Xi J, Wang T, Xian P, Liu X, Du M, Yang H, Palanisamy CP, Lin W, Long Q. Proteomic insights uncover enhanced neurotherapeutic potential in conditioned mesenchymal stem cell-derived extracellular vesicles. Extracellular Vesicle. 2024; 3: 100037.
[29] Pei J, Natarajan PM, Umapathy VR, Swamikannu B, Sivaraman NM, Krishnasamy L, Palanisamy CP. Advancements in the synthesis and functionalization of zinc oxide-based nanomaterials for enhanced oral cancer therapy. Molecules. 2024; 29(11): 2706.
[30] Gatasheh MK, Natarajan SR, Krishnamoorthy R, Alsulami TS, Rajagopal P, Palanisamy CP, Veeraraghavan VP, Jayaraman S. Molecular analysis to identify novel potential biomarkers as drug targets in colorectal cancer therapy: an integrated bioinformatics analysis. Molecular and Cellular Oncology. 2024; 11(1): 2326699.
[31] Pei J, Yan Y, Jayaraman S, Rajagopal P, Natarajan PM, Umapathy VR, Gopathy S, Roy JR, Sadagopan CS, Thalamati D, Palanisamy CP, Mironescu M. A review on advancements in the application of starch-based nanomaterials in biomedicine: Precision drug delivery and cancer therapy. International Journal of Biological Macromolecules. 2024; 130746.
[32] Pei JJ, Yan Y, Palanisamy CP, Jayaraman S, Natarajan PM, Umapathy VR, Gopathy S, Roy JR, Sadagopan JC, Thalamati D, Mironescu M. Materials-based drug delivery approaches: Recent advances and future perspectives. Green Processing and Synthesis. 2024; 13: 20230094.
[33] Pei JJ, Deng W, Liu Y, Guo Y, Chen J, Abdu H, Khan MR, Palanisamy CP, El-Aty AM. A Comprehensive Review of Cornus officinalis: Health Benefits, Phytochemistry, and Pharmacological Effects for Functional Drug and Food Development. Frontiers in Nutrition. 2023; 10: 1309963.
[34] Natarajan PM, Umapathy VR, Murali A, Swamikannu B. (2022). Computational Simulations of Identified marine-derived Natural Bioactive Compounds As Potential Inhibitors of Oral Cancer. Future Science OA. 2022; 8(3).

[35] Natarajan PM, Umapathy VR. Role of transcriptomics in the study of oral cancer. Frontiers in Oral Health. 2025; 6:1524364.
[36] Vidhyarekha U, Natarajan PM, Bhuminathan S, Sabarinathan J, Suba R, Vijayalakshmi P. Role of artificial intelligence in Oral Cancer. Advances in Public Health. 2024. 2024: 3664408.
[37] Ganesan A, Kumar NG, Natarajan PM, Gauthaman J. Automated classification of elongated styloid processes using deep learning models-an artificial intelligence diagnostics. Frontiers in Oral Health. 2025; 5: 1424840.
[38] Umapathy VR, Natarajan PM, Swamikannu B. Regenerative Strategies in Dentistry: Harnessing Stem Cells, Biomaterials and Bioactive Materials for Tissue Repair. Biomolecules. 2025; 15: 546.
[39] Natarajan PM. Dental Bioinformnatics-Current Scope and Future perspectives. Research Journal of Pharmacy and Technology. 2022;15(5):2351-6.
[40] Ganesan A, Kumar NG, Natarajan PM. Solanum trilobatum leaf extract-derived silver nanoparticles downregulate the PI3K/AKT/mTOR signaling pathway and attenuate oral squamous cell carcinoma cell proliferation. Journal of Herbmed Pharmacology. 2024; 13(2): 300-307.
[41] Perumal MKK, Renuka RR, Subbiah SK, Natarajan PM. Artificial intelligence-driven clinical decision support systems for early detection and precision therapy in oral cancer: a mini review. Frontiers in Oral Health. 2025; 6: 1592428.
[42] Ramesh E, Ganesan A, Lakshmi KC, Natarajan PM. Artificial intelligence-based diagnosis of oral leukoplakia using deep convolutional neural networks Xception and MobileNet-v2. Frontiers in Oral Health. 2025; 6: 1414524.
[43] Daniel Raja FS, Abraham L, Rangasamy K, Saikia K, Rathankumar AK, Mironescu M, Mironescu I, Palanisamy CP, Kanniappan GV. Next-Generation Microbiome Therapeutics: Psychobiotics and Fecal Microbiota Transplants (FMT) for Mental Health Treatment. Frontiers in Cellular and Infection Microbiology. 2026; 16: 1719357.
[44] Dharmaprakash S, Gunasekaran VP, Sivaramakrishnan R, Kanniappan GV, Jayaraman S, Mironescu M, Rajabathar JR, Mironescu ID, Palanisamy CP. Marine macroalgae-mediated ultrasonic-assisted green synthesis of CuO nanoparticles embedded in starch/PVA electrospun nanoscaffolds for in vitro α-amylase and α-glucosidase inhibitory activity. Scientific Reports. 2026.
[45] Surendran N, Chandrasekaran G, Raju MV, Chandrasekaran MK, Ahalliya RM, Palanisamy CP, Kanniappan GV, Arcot R, Alharbi NS, Thiruvengadam M. Anti-inflammatory potential of ethanolic extract of Maranta arundinacea L.: Insights from COX-2 modulation and oxidative stress analysis. South African Journal of Botany. 2026; 195: 142-151.
[46] Pei J, Senthilkumar MV, Hessini K, Subramaniyam S, Sivaramakrishnan R, Kanniappan GV, Jayaraman S, Palanisamy CP. Green fabrication of starch/PVA/CuO nanoscaffolds using marine macroalgae extract for enhanced anti-inflammatory activity. Sustainable Chemistry and Pharmacy. 2026; 51: 102397.
[47] Balasubramanian V, Loganathan L, Muthuswamy K, Viswanathan TM, Raju MV, Chandrasekaran MK, Ahalliya RM, Poorasamy J, Palanisamy CP, Dominic S, Kanniappan GV. Anticancer therapeutic efficacy of PEGylated β-galactosidase from Aspergillus terreus in DMBA-induced breast cancer: Toxicological, molecular and histopathological evaluation in Wistar rats. International Journal of Biological Macromolecules. 2026; 360: 151856.
[48] Jayaraman S, Eswaran A, Rajagopal P, Palanisamy CP, Veerakumar P, Veeraraghavan VP, Sirasanagandla SR. Neuroendocrine-associated epigenetic factors in cellular senescence: mechanisms and therapeutic implications. Biogerontology. 2026; 27(2): 64.
[49] Ponnusamy B, Rajagopal P, Palanisamy CP, Veeraraghavan VP, Jayaraman S. Mechanistic Exploration of the anticancer activity of Justicia adhatoda Plant Leaf Ethanolic Extract against Colon Cancer Cells: An in silico and in vitro Approach. Asian Pacific Journal of Cancer Prevention. 2026; 27(3): 1069-1080.
[50] Pei J, Saran VS, Sivaramakrishnan R, Kanniappan GV, Pandurangan V, Jayaraman S, Dhayalan VK, Mironescu M, Mironescu ID, Palanisamy CP. Ultrasonic-assisted, Sargassum ilicifolium (brown marine macroalgae)-mediated biogenic synthesis of CuO nanoparticles incorporated in starch/PVA electrospun nanoscaffolds: In vitro safety and antioxidant efficacy assessment. Bioorganic Chemistry. 2026; 173: 109679.
[51] Raj MAPA, Subramaniyam S, Kanniappan GV, Jayaraman S, Palanisamy CP. Sustainable fabrication of starch/PVA/CuO electrospun nanoscaffolds from Turbinaria ornata (marine macroalgae) extract: Physicochemical characterization and antidiabetic evaluation. Kuwait Journal of Science. 2026; 53(2): 100545.
[52] Pei J, Ganesh NS, Subramaniyam S, Sivaramakrishnan R, Kanniappan GV, Jayaraman S, Palanisamy CP. Sustainable fabrication of starch/PVA/CuO electrospun nanoscaffolds from Padina tetrastromatica (Brown macroalgae) extract: Physicochemical characterization and antidiabetic assessment. Sustainable Chemistry One World. 2026; 9: 100195.
[53] Sakthiraj A, Sivaramakrishnan R, Subramaniyam S, Kanniappan GV, Pandurangan V, Jayaraman S, Dhayalan VK, Mironescu M, Mironescu ID, Palanisamy CP. Starch/PVA electrospun nanoscaffolds loaded with ultrasonic-assisted green-synthesis of CuO nanoparticles from marine macroalgae (Gracilaria corticata) extract: Cytotoxicity and antioxidant analysis. Chemical Physics Impact. 2026; 12: 101018.

[54] Raju M, Chandrasekaran MK, Loganathan L, Ahalliya RM, Mironescu M, Mironescu ID, Palanisamy CP, Kanniappan GV. Lipid remodeling and ferroptosis in phosphatidylcholine-mediated tumor–stroma crosstalk. Frontiers in Molecular Biosciences. 2026; 13: 1742305.
[55] Kunamalla R, Panagal M, Palanisamy CP. Biogenic synthesis and fabrication of starch/PVA/CuO electrospun nanoscaffolds from Sargassum ilicifolium (brown marine macroalgae) extract for anticancer activity on HT-29 and MCF-7 cancer cells. Biocatalysis and Agricultural Biotechnology. 2026; 72: 103923.
[56] Pei J, Govindaraj H, Sivaramakrishnan R, Kanniappan GV, Pandurangan V, Dhayalan VK, Mironescu M, Mironescu ID, Jayaraman S, Palanisamy PC. Sustainable fabrication of biopolymer-based (starch/PVA) nanoscaffolds loaded with green-synthesized CuO nanoparticles from Sargassum wightii (marine macroalgae): Cytocompatibility and antioxidant activity. Biomaterials Advances. 2026; 182: 214660.
[57] Pei J, Perumal NC, Meng P, Long Q, Palanisamy CP. Extracellular vesicle-based biosensors for Alzheimer's disease: A new frontier in precision diagnostics. Ageing Research Reviews. 2026; 113: 102904.
[58] Shree P, Sivaramakrishnan R, Kanniappan GV, Pandurangan V, Jayaraman S, Dhayalan VK, Mironescu M, Mironescu ID, Palanisamy CP. Antioxidant and biocompatible CuO-starch/PVA nanoscaffolds via ultrasonic green synthesis using Turbinaria conoides (brown marine macroalgae). Medicine in Drug Discovery. 2025; 28: 100238.
[59] Gong J, Lin J, Guan T, Pei J, Palanisamy CP, El-AtyFrom AMA. selenium tolerance to nanoplastic antagonism: Comprehensive characterization of L. casei SNUT1 and its extracellular vesicle–nanoselenium complex. Food Bioscience. 2025; 74: 107749.
[60] Poochi SP, Sundarraj R, Raju MV, Chandrasekaran MK, Ahalliya RM, Palanisamy CP, Kanniappan GV, Kondapavuluri BK, Thiruvengadam M. Harnessing Nature: Computational and Experimental Insights Into *Ipomoea obscura* Metabolites for Bladder Cancer Therapy. Chemistry and Biodiversity. 2025; 0: e00909.
[61] Dugganaboyana GK, Kannankumar MKG, Shivaramakrishna S, Raju MV, Chandrasekaran MK, Ahalliya RM, Panneerselvam N, Palanisamy CP, Kanniappan GV. Phytochemical insights, antioxidant activity and therapeutic potential of Cassia senna against prostate cancer in Wistar albino rats. Discover Applied Sciences. 2025; 7:1206.
[62] Natarajan SR, Krishnamoorthy R, Alshuniaber MA, Gatasheh MK, Rajagopal P, Veeraraghavan VP, Palanisamy CP, Jayaraman S. KDM1A Facilitates Oncogenic Potential in Colorectal Cancer Progression Through the Activation of AXIN/GSK3β/β-Catenin Signaling Pathways: Evidence From Integrated Transcriptomics and In Vitro Studies. The Journal of Gene Medicine. 2025; 27(11): e70053.
[63] Guan T, Gong J, Lin J, Palanisamy CP, Jinjin Pei J, El-Aty AMA. Machine learning-driven multimodal optimization of selenium biotransformation and flavor profiling in fermented apple–Yacon functional beverages. Innovative Food Science & Emerging Technologies. 2025; 105: 104198.
[64] Natarajan SR, Krishnamoorthy R, Alshuniaber MA, Alsulami TS, Gatasheh MK, Rajagopal P, Palanisamy CP, Govindan R, Veeraraghavan VP, Jayaraman S. ABCE1 facilitates tumour progression via aerobic glycolysis and inhibits cell death in human colorectal cancer cells through the p53 signalling pathway. Scientific Reports. 2025; 15: 24674.
[65] Huang Y, Guo H, Liu Y, Jin W, Palanisamy CP, Pei J, Oz F, El-Aty AMA. Effects of Natural Polysaccharides on the Gut Microbiota Related to Human Metabolic Health. Molecular Nutrition & Food Research. 2025; 69:e202400792.
[66] Poornima K, Meenakshi K.C, Manikandan V.R, Shankari G, Prabhu D, Rathi M.A, Palanisamy CP, Balaji R, Gopalakrishnan V.K. Exploring the anticancer potential of Jerantinine A from *Tabernaemontana coronaria* against prostate, breast, and ovarian cancers: A computational approach. *Journal of Complementary and Integrative Medicine*, 2025 22(2): 363–372.
[67] Palanisamy CP, Poompradub S, Sansanaphongpricha K, Jayaraman S, Subramani K. Faridah Sonsudin gGreen synthesis of Nigella sativa-mediated silver nanoparticles for enhanced antibacterial activity and wound healing: Mechanistic insights and biomedical applications. Environmental Nanotechnology, Monitoring & Management. 2025; 24: 101085.
[68] Alugoju P, Palanisamy CP, Anthikapalli NVA, Jayaraman S, Prasanskulab A, Chuchawankul S, Dyavaiah M, Tencomnao T. Exploring the anti-aging potential of natural products and plant extracts in budding yeast Saccharomyces cerevisiae: A review. F1000Research. 2023; 12: 1265.
[69] Lavanya M, Krishnamoorthy R, Alshuniaber MA, Manoharadas S, Palanisamy CP, Veeraraghavan VP, Jayaraman S, Rajagopal P, Padmini R. Formulation, characterization and evaluation of gelatin-syringic acid/zinc oxide nanocomposite for its effective anticancer, antioxidant and anti-inflammatory activities. Journal of King Saud University-Science. 2023; 35: 102909.